Energy integral description of the development of Kelvin-Helmholtz billows

By J. T. C. LIU and L. MERKINE,[1] *Brown University, Providence, Rhode Island 02912, USA*

(Manuscript received May 27; in final form August 26, 1975)

ABSTRACT

In this paper we study the development of instability waves in a stratified shear flow which occurs, for instance, in frontal zones and on large scale internal waves where the Richardson number is sufficiently low. The model is based on splitting the flow into the mean flow and instability wave components. The basis for the interaction between the mean flow and the wave is their respective vertically integrated energy flux equations. The wave description is obtained through a shape assumption: the time dependent wave amplitude is determined by its energy equation solved jointly with the mean flow and the vertical shape function is given by the local linear theory. The instability wave kinetic energy development is determined by the balance between energy production from the mean flow and the conversion of fluctuation kinetic to potential energy. From the energy integral considerations, the numerical results show moderately good agreement with observations in our estimate of the lifetime of the wave and the doubling of the thickness of the mean shear layer during this time. The modification of the mean flow velocity and temperature profiles is explained via the effects of the wave generated vertical momentum and heat (or buoyancy) fluxes, respectively.

1. Introduction

Since the 1961 Farnborough conference on atmospheric turbulence and its relation to aircraft operations, at least five international conferences have been held dealing with various meteorological aspects of the subject. Several reviews have also appeared (Dutton, 1971; Lilly, 1971). It is now recognized and generally established that Kelvin-Helmholtz instability, in its nonlinear rather than linear stages, is one of the important sources of "clear-air turbulence". It is most likely to occur in regions of concentrated baroclinicity where vertical wind shear and static stability are strong and the appropriate Richardson number small. Observations in the atmosphere have brought about this conclusion. These include cloud observations (Ludlam, 1967; Scorer, 1972), pulsed radar observations using small inhomogeneities of the refractive index in the instability as a tracer (Browning, 1971; Browning & Watkins, 1970; Hardy et al., 1966; Hardy et al., 1969; Hicks & Angell, 1968), FM–CW radar observations at vertical incidence (Atlas et al., 1970); aircraft observations (Axford, 1970; 1973; Mather, 1971), and joint radar, radiosonde and aircraft observations (Browning et al., 1973; Hardy et al., 1973; Metcalf & Atlas, 1973). Instabilities of the Kelvin-Helmholtz type have also been found in the ocean (Woods, 1968; Woods & Wiley, 1972) in regions where current shear and static stability are present. In such regions, the ocean microstructure (Cox et al., 1969) is thought to be the result of Kelvin-Helmholtz instabilities (Woods & Wiley, 1972; Munk & Garrett, 1973), and is now thought to be of great importance to the vertical mixing processes in the ocean (Woods, 1972), at least in regions where such instabilities play the dominant role. Finally, more detailed observations of the nonlinear development of the Kelvin-Helmholtz instability have been made under laboratory conditions (Thorpe, 1971; 1973*a*, 1973*b*).

Our interest is in obtaining some theoretical understanding of the events in the *life cycle* of

[1] Present address: Department of Meteorology, Massachusetts Institute of Technology, Cambridge, Massachusetts.

the observed Kelvin-Helmholtz billows, now thought to be important to the mixing processes in the atmosphere and the ocean. In order to fix our ideas we first review some of the details of one of the clearest observations of Kelvin-Helmholtz wave *development* in the atmosphere (Browning & Watkins, 1970). In this case, simultaneous observations by steerable highpower radar and radiosonde established the life cycle of the instability which occurred within a frontal zone. At the beginning a clear-air echo layer less than 150 m in vertical thickness was embedded in a stable layer of about 800 m in vertical extent. Radiosonde measurements over a 200 m depth were used to deduce the layer Richardson number, which was nearly 1/4 for 600 m depth. The echo layer acted as a tracer for the large-scale instability. Instabilities developed, as observed by radar, with crest-to-trough amplitude growing to 300 to 400 m with wave lengths of 3 to 5 km. The local wave number, made dimensionless by the half-layer thickness, was thus about 0.5–0.8, not far removed from 0.5 predicted by the linear theory for the most amplified disturbances for Richardson number below 1/4 (see, for instance, Maslowe & Kelly, 1971). In subsequent developments the radiosonde observations showed that the potential temperature gradient decreased at and increased away from the center. Thus, in effect, the splitting of the original strong static stability layer appeared simultaneously with the active development of the Kelvin-Helmholtz instability. Radar observations indicated that the subsequent double echo layer corresponded to the vertical location of the split stability layer. However, the wind shear profiles did not show a splitting, but decreased slightly throughout the layer. Total development time of the active large-scale instability was about 15–20 minutes at which time the shear layer doubled its original thickness. The radiosonde measurements of layer Richardson number (an elusive parameter) over vertical depths of 200 m could conceivably be sufficiently coarse to obscure the more relevant Richardson numbers at smaller scales. For instance, it would be difficult to obtain the layer Richardson number of the original echo layer of less than 150 m. However, from the evidence which already exists here and in other observations, it is not difficult to conclude that the instability wave developed out of the Kelvin-Helmholtz instability of the linear theory for the appropriate Richardson number less than 1/4 and a wave number which correspond to the most amplified mode.

In order to study the development or life cycle of the Kelvin-Helmholtz billows, we extend the technique for homogeneous shear flows (Ko et al., 1970; Liu & Lees, 1970; Liu & Gururaj, 1974) to a stratified shear flow. From detailed observations in homogeneous shear flows, the appearance of instability waves in such flows coincided with large distortions of the mean flow as the instability develops into finite amplitude. The mean flow and the developing instability interacts strongly and a formulation based on integrated energy equations of both components provide an overall description of the interaction. The details of the formulation and results for homogeneous shear flows are discussed in Ko et al., (1970), Liu & Lees (1970) and Liu & Gururaj (1974). The extension of the energy integral consideration to the stratified shear layer problem, with application to observations in geophysical problems, is discussed in this paper.

2. Formulation of the nonlinear problem

Concentrated shear and stability layers are observed to occur over large horizontal distances and are nearly two-dimensional. For simplicity, we assume that the shear vector maintains a constant orientation with height and take the basic mean flow to be identically two-dimensional and (quasi-)steady. The basic mean flow and its nomenclature are shown in Fig. 1: the total velocity difference ΔU is $2U_1$, the initial half-layer thickness is δ_{u1}, and vertical coordinate z is measured from the center of the shear layer. For such a mean flow, as in the experimental arrangement of Thorpe (1971) in the laboratory and Browning & Watkins (1970) in the atmosphere, an individual billow, after its natural initiation, can be followed and its life cycle studied. However, the vertical extent of the billow here is not bounded by walls as would be in the laboratory case. The clear echo layer observed by radar during the billow development is due to oscillations of small-scale inhomogeneities, perhaps orderly rather than random, which do not fill the entire shear layer (Browning et al., 1973). Thus, the basic shear

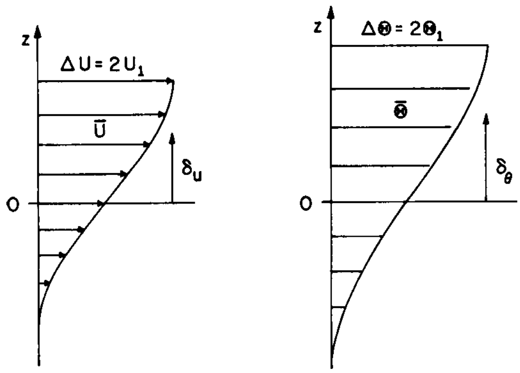

Fig. 1. Schematic of the velocity shear and potential temperature layers.

layer growth is more likely to be due to the direct effect of the large amplitude Kelvin-Helmholtz instability than to the small amplitude, small-scale oscillations. On the other hand, had the small-scale oscillations been found to fill the entire shear layer, the situation would be different, in which case the energetic exchanges between the mean motion, wave and small scale oscillations would be of importance, and the problem would then be that of a large eddy developing in a turbulent shear flow. We here regard the small-scale oscillations as tracers and neglect the energetic exchange processes of the small-scale structure with both the mean flow and the instability wave. This necessarily limits our consideration up to the breakdown of the billow. Also, the scale of the wave motion is sufficiently large that we consider the problem to be inviscid and nonconducting. The physical problem is one of nonlinear development of *dynamically* unstable waves in a stably-stratified shear flow. Other assumptions which lead to our starting point are that for the scales of motion of interest the Coriolis force can be neglected, the reference state is hydrostatic and adiabatic, and the Boussinesq approximation is used. The basic equations may be found, for instance, in Lumley & Panofsky (1964).

The dimensionless form of the basic equations for quantities that are departures from the hydrostatic state are

$$\text{continuity:}\quad \frac{\partial U_j}{\partial x_j} = 0 \tag{1}$$

$$\text{momentum:}\quad \frac{\partial U_i}{\partial t} + \frac{\partial U_i U_j}{\partial x_j} = -\frac{\partial P}{\partial x_i} + \mathrm{Ri}\,\Theta\,\delta_{3i} \tag{2}$$

$$\text{energy:}\quad \frac{\partial \Theta}{\partial t} + \frac{\partial U_j \Theta}{\partial x_j} = 0 \tag{3}$$

where the dimensionless velocities U_j are referred to $U_1 = \Delta U/2$ (see Fig. 1), potential temperature Θ to $\Theta_1 = \Delta\Theta/2$, pressure P to $\varrho_0 U_1^2$, ϱ_0 being the hydrostatic density at the appropriate height concerned, the dimensionless coordinates are referred to the *initial* velocity half-layer thickness δ_{u1}, time t to δ_{u1}/U_1, and the layer Richardson number is $\mathrm{Ri} = g\Theta_1\delta_{u1}/\Theta_0 U_1^2$, where Θ_0 is the potential temperature of the hydrostatic state and g the gravitational acceleration. Both ϱ_0 and Θ_0 are taken as constants appropriate to the height concerned in the Boussinesq approximation, δ_{3i} is the Kronecker delta, $i = 1$ and 3 are the horizontal and vertical directions, respectively, and x_i is denoted by x, z.

In order to analyze the instability wave development, we split any total flow quantity $Q(x, z, t)$ into a basic mean quantity $\bar{Q}(z, t)$, which is horizontally homogeneous and a fluctuation quantity $q(x, z, t)$ which is horizontally periodic with zero mean,

$$\begin{aligned} U &= \bar{U} + u,\\ W &= 0 + w,\\ P &= \bar{p} + p,\\ \Theta &= \bar{\Theta} + \theta \end{aligned} \tag{4}$$

where U and W are the horizontal and vertical velocities, respectively. The horizontal average referred to above is taken over one billow wave length. Substitution of eq. (4) into eqs. (1)–(3) and subsequent horizontal averaging, denoted by an overbar, produces the following mean flow equations:

$$\frac{\partial \bar{U}}{\partial t} = \frac{\partial(-\overline{uw})}{\partial z} \tag{5}$$

$$\frac{\partial \bar{p}}{\partial z} = \frac{\partial(-\overline{w^2})}{\partial z} + \mathrm{Ri}\,\bar{\Theta} \tag{6}$$

$$\frac{\partial \bar{\Theta}}{\partial t} = \frac{\partial(-\overline{w\theta})}{\partial z} \tag{7}$$

The mean flow is modified through the wave contributions to momentum and heat fluxes as the wave motion amplifies into large amplitudes. Such interactions will be "permanent" impressions left on the mean motion by the finite amplitude instability wave long after the wave has decayed, unless other subsequent stirring motions (which are not considered here) alter this. We note that there is no *net* momentum and heat flux according to eqs. (5) and (7).

The instantaneous, nonlinear conservation equations for the disturbance quantities are obtained by subtracting the mean flow equations (5)–(7) from the total equations (1)–(3). The equations for the averaged disturbance correlations appearing in (5)–(7) are obtained by forming such products from the instantaneous quantities and then averaging. However, this will lead to triple correlation quantities as in the turbulence problem, and one faces similar closure questions. The disturbance quantities under the average signs here, however, are developed from the Kelvin-Helmholtz instability; thus *ad hoc* relationships between the correlations and the mean flow are neither desirable nor warranted for the purpose of our analysis. Rather than attempting to solve the problem "exactly" on a point-to-point basis, we shall make use of the integral forms of the conservation equations, in this case averaged vertically. We then seek the time evolution of vertically-averaged energetic quantities. In order to do this we also need to make the shape assumptions for the vertical distribution of physical quantities with certain time-dependent parameters which are then determined by the vertically-averaged conservation equations. The problem is thus reduced from partial to ordinary differential equations in time only. The technique is essentially similar to one introduced in boundary-layer theory by von Kármán (1921). Such a technique for finite-amplitude instability problems was discussed by Stuart (1958) for parallel shear flows, and more recently it has been extended to problems in a homogeneous fluid for developing shear layers where good agreement has been found with some of the details of laboratory experiments (Ko et al., 1970; Liu & Lees, 1970; Liu & Gururaj, 1974). It is thus of advantage to consider our present problem in this light, particularly because we are interested in the time evolution of the billow and mean flow interactions.

(a) Vertically integrated conservation equations

To proceed, the basis of the wave description, in particular its amplitude development, is here taken to be given by the averaged kinetic energy equation for the wave

$$\frac{\partial \overline{q^2}/2}{\partial t} = -\overline{uw}\frac{\partial \bar{U}}{\partial z} - \mathrm{Ri}\,(-\overline{w\theta}) - \frac{\partial}{\partial z}(\overline{wq^2}/2 + \overline{wp}) \tag{8}$$

where $q^2 = u^2 + w^2$. The wave kinetic energy increases, on the average, because of the energy transfer from the mean motion represented by the first term in eq. (8); the second term represents conversion from kinetic to potential energy, and the last term is the "diffusion" of wave energy by the vertical motions of the wave itself. The kinetic energy equation for the mean flow is obtained from (5):

$$\frac{\partial \bar{U}^2/2}{\partial t} = -(-\overline{uw})\frac{\partial \bar{U}}{\partial z} - \frac{\partial \bar{U}\,\overline{uw}}{\partial z} \tag{9}$$

Similarly, the equation for $\bar{\Theta}^2$ is obtained from (7):

$$\frac{\partial \bar{\Theta}^2/2}{\partial t} = -(-\overline{w\theta})\frac{\partial \bar{\Theta}}{\partial z} - \frac{\partial \bar{\Theta}\,\overline{w\theta}}{\partial z} \tag{10}$$

The vertically integrated forms of eqs. (8)–(10) are obtained, following von Kármán (1921) by integrating over a *finite* region occupied by the shear layer,

$$\frac{1}{2}\frac{d}{dt}\int_{-\infty}^{\infty}\overline{q^2}\,dz = \int_{-\infty}^{\infty}(-\overline{uw})\frac{\partial \bar{U}}{\partial z}\,dz - \mathrm{Ri} \times \int_{-\infty}^{\infty}(-\overline{w\theta})\,dz \tag{11}$$

$$\frac{1}{2}\frac{d}{dt}\left[\int_{-\infty}^{0}(\bar{U}^2 - \bar{U}^2_{-\infty})\,dz + \int_{0}^{\infty}(\bar{U}^2 - \bar{U}^2_{\infty})\,dz\right] = -\int_{-\infty}^{\infty}(-\overline{uw})\frac{\partial \bar{U}}{\partial z}\,dz \tag{12}$$

$$\frac{1}{2}\frac{d}{dt}\left[\int_{-\infty}^{0}(\bar{\Theta}^2 - \bar{\Theta}^2_{-\infty})\,dz + \int_{0}^{\infty}(\bar{\Theta}^2 - \bar{\Theta}^2_{\infty})\,dz\right] = -\int_{-\infty}^{\infty}(-\overline{w\theta})\frac{\partial \bar{\Theta}}{\partial z}\,dz \tag{13}$$

Because of entrainment, the shear layer region develops in time. The interchange of the time derivative and the integration for eqs. (12) and (13) introduces the dimensionless velocities $\bar{U}_{\pm\infty}$ and temperature $\bar{\Theta}_{\pm\infty}$ at the upper and lower edges of the shear and temperature layers. Because the integrand of eqs. (12) and (13) vanishes at the outer edges of the shear and temperature layers, the limits of integration are then taken to $\pm\infty$. Both $\bar{U}_{\pm\infty}$ and $\bar{\Theta}_{\pm\infty}$ are taken as uniform and equal to 2 and 0 at the upper and lower edges, respectively. Implicit in the above is that in obtaining (11)–(13) we assume that the disturbances vanish far away from the shear layer.

(b) Shape assumptions for the integral problem

The mean motion, through its interaction with the Kelvin-Helmholtz wave, determines the growth of the velocity shear and potential temperature layers and the amplitude of the instability wave. Such nonlinear interactions follow from eqs. (11)–(13), which must be supplemented by the shape assumptions for the mean and disturbance quantities. The overall quantities, such as the dimensionless half-shear layer thickness $\delta_u(t)$ (referred to its initial value δ_{u1}), half-potential temperature layer thickness $\delta_\theta(t)$ (also referred to δ_{u1}), and the disturbance amplitude function $|A(t)|^2$ are not sensitive to the details of the shape distributions. We can write the mean flow quantities as

$$\bar{Q}(\zeta, t) = Q_l(\zeta) + Q_m(\zeta, t)$$

where Q_l is the basic mean flow quantity and $\zeta = z/\delta_u$. Here $Q_m = 0(|A|^2)$, which is in some sense small, so that $Q_l(\zeta)$ is a good first approximation for the mean profiles in eqs. (11)–(13). The permanent distortion of the details of the mean flow is given by Q_m and is obtained via momentum and buoyancy flux considerations, (5) and (7) respectively, after the overall mean motion and disturbance problems are solved through (11)–(13), this will be discussed in conjunction with the numerical results. To be specific, we take the first approximation to the basic mean flow to be given by

$$U_l(\zeta) = \tanh \zeta + 1 \tag{14}$$

$$\Theta_l(\zeta r) = \tanh \zeta r + 1 \tag{15}$$

where $r = \delta_u/\delta_\theta$. The mean motion is thus characterized by δ_u and r or equivalently δ_θ. The usual way of defining δ_u and δ_θ is that for a fixed value of $\zeta = z/\delta_u$, U_l and Θ_l becomes a certain fixed fraction of their respective values at the outer edges for all times. For instance, if $\zeta = \pm 1$ and $\zeta r = \pm 1$ in (14) and (15), then $U_l(1)$ and $\Theta_l(1)$ equal 1.76 ($U_{+\infty}$ and $\Theta_{+\infty} = 2$).

We do not consider here how such a basic mean flow is generated but assume that it existed initially on the mesoscale (Browning & Watkins, 1970), in frontal systems, for example; in the laboratory it is set up via molecular diffusion (Thorpe, 1971). It is only the subsequent dynamics, or energetics, that we deal with. The disturbance distribution, following earlier works (for instance, Liu & Lees, 1970), is taken to be described by a *local* linear theory but suitably modified by an unknown amplitude function, $A(t)$. As Thorpe (1971) has shown in the laboratory, "natural" disturbances originate and develop at below-critical Richardson numbers and take on a wave number, made dimensionless by half the initial layer thickness, corresponding to the most amplified case. For spatially periodic and time-amplifying disturbances, the physical wave number remains fixed. We thus consider a single fundamental component at a fixed physical wave length; and let

$$\begin{bmatrix} u(\xi, \zeta, t) \\ w(\xi, \zeta, t) \\ \theta(\xi, \zeta, t) \end{bmatrix} = A(t) \begin{bmatrix} \phi'(\zeta; \alpha, \mathrm{Ri}\, \delta_u r) \\ -i\alpha\phi(\zeta; \alpha, \mathrm{Ri}\, \delta_u r) \\ \tau(\zeta; \alpha, \mathrm{Ri}\, \delta_u r) \end{bmatrix} \times \exp(i\alpha\xi) + \text{c.c.} + O(A^2) \tag{16}$$

where c.c. denotes complex conjugate. The vector on the left hand side of eq. (10) is thus twice the real part of the vector on the right hand side. The instability quantities occurring in the subsequent integrals are in terms of energy and the integrands are all real.

Prime refers to differentiation with respect to ζ. In the *local* linear theory, $\xi = x/\delta_u$ and the dimensionless real wave number α is $\alpha_1\delta_u$, where α_1 is fixed and measured in units of δ_{u1}. The eigenfunctions of the fundamental components ϕ and τ correspond to the disturbance streamfunction and temperature, respectively, and are presumed known (but must be solved locally). The linear theory (see, for instance, Maslowe & Kelly, 1971) gives

$$\begin{gathered} \phi'' - [\alpha^2 - U_l''/(U_l - c) - \mathrm{Ri}\, \delta_u r \Theta_l'/(U_l - c)^2]\phi = 0, \\ \tau = \Theta_l'\phi/(U_l - c), \\ \phi \text{ and } \tau \to 0 \text{ as } |\zeta| \to \infty \end{gathered} \tag{17}$$

where c is the complex wave speed. The eigenfunctions are obtained for given U_l and Θ_l and for each value of the parameters $\mathrm{Ri}\delta_u r$ and α. Since ϕ is determined only to a multiplicative (local) constant, we attribute physical meaning to $|A|^2$ by normalizing ϕ so that

$$\int_{-\infty}^{\infty} (|\phi'|^2 + \alpha^2|\phi|^2)\, d\zeta = 1 \tag{18}$$

Thus $|A|^2$ may be interpreted as the integrated kinetic energy of the wave, averaged over one wave length, across the shear layer per unit δ_u. The quantity that characterizes the wave development is $|A(t)|^2$, and this must be determined jointly with δ_u and δ_θ in the overall nonlinear interaction problem.

(c) The nonlinear interaction problem

Upon substitution of eqs. (14)–(16) into (11)–(13), we obtain three corresponding equations

$$\frac{d\delta_u|A|^2}{dt} = |A|^2 I_{rs}(t) - |A|^2 \mathrm{Ri}\, \delta_u I_{wt}(t) \tag{19}$$

$$\frac{d\delta_u}{dt} = |A|^2 I_{rs}(t) \tag{20}$$

$$\frac{d\delta_\theta}{dt} = |A|^2 r(t)\, I_{hf}(t) \tag{21}$$

with initial values $t=0$: $\delta_u = 1$, $\delta_\theta = r_1$, $|A|^2 = |A|_0^2$.

The terms on the right-hand sides of eqs. (19)–(21) correspond to those of (11)–(13) respectively. The integrals defined are

$$I_{rs}(t) = \int_{-\infty}^{\infty} i\alpha(\phi\tilde{\phi}' - \tilde{\phi}\phi')\, \mathrm{sech}^2\, \zeta\, d\zeta \tag{22}$$

$$I_{hf}(t) = \int_{-\infty}^{\infty} i\alpha(\phi\tilde{\tau} - \tilde{\phi}\tau)\, \mathrm{sech}^2\, r\zeta\, d\zeta \tag{23}$$

$$I_{wt}(t) = \int_{-\infty}^{\infty} i\alpha(\phi\tilde{\tau} - \tilde{\phi}\tau)\, d\zeta \tag{24}$$

where the tilde denotes the complex conjugate. The integrals (22)–(24) are all positive quantities in this problem since we are dealing with a growing unstable wave performing work against gravity. The signs of these integrals are also borne out from subsequent numerical results. They are of order unity, but approach zero as the local linear problem approaches the neutral curve when energy is no longer being drawn from the mean flow. Equations (19)–(21) are three coupled nonlinear first-order equations describing the time evolution of δ_u, δ_θ and $|A|^2$. It is instructive to recast eq. (19) into the form

$$\frac{d|A|^2}{dt} = \frac{1}{\delta_u}\left(|A|^2(I_{rs} - \mathrm{Ri}\, \delta_u I_{wt}) - |A|^4 I_{rs}\right] \tag{25}$$

with the use of eq. (20). In the initial stages when $|A|^2$ is relatively small, eqs. (20) and (21) tell us that δ_u and δ_θ are very nearly constant and eq. (25) tells us that $|A|^2$ grows exponentially with time with a growth factor $[I_{rs}(0) - \mathrm{Ri}\, I_{wt}(0)] \simeq 2\alpha C_i$, which is determined by the linear theory. When the disturbance amplifies to sufficiently large magnitude, the growth rate is governed by eq. (25) (and not by the local linear theory). The integrals I_{rs} and I_{wt} decrease rapidly with increasing δ_u until they approach zero as the local linear theory approaches the neutral curve. In that situation, both this time dependency of the integrals and the $|A|^4$ term in eq. (25) limit the growth of $|A|^2$.

3. Numerical application and comparison with observations

Prior to discussing the numerical application, some discussion of the ranges of parameters chosen and the relation to observations are first warranted. The initial-layer Richardson number defined in Sec. 2, $\mathrm{Ri} = g\Theta_1\delta_{u1}/\Theta_0 U_1^2$, can also be written as $\mathrm{Ri} = g\Delta\Theta(2\delta_{u1})/\Theta_0(\Delta U)^2$ in terms of the total differences of velocity and potential temperature and the total layer thickness. In order to proceed with the numerical application of the problem, we need to obtain a value of Ri which approximates those observed. From Woods & Wiley's (1972) observations in the Mediterranean thermocline, the typical sheet thickness is $2\delta_{u1} \simeq 10^{-1}$ m, the velocity difference $\Delta U \simeq 2.2 \times 10^{-2}$ m/s and the fractional density difference about 2×10^{-5}. This gives the appropriate $\mathrm{Ri} \simeq 0.04$. In the laboratory (Thorpe, 1971, 1973*a*, 1973*b*), $\mathrm{Ri} \simeq 0.05$. From atmospheric observations, for instance (Browning & Watkins, 1970), the onset of Kelvin-Helmholtz instability is also definitely associated with low Richardson numbers although the initial shear layer thickness in our context is difficult to estimate. In our calculations, we take $\mathrm{Ri} = 0.08$. Furthermore, laboratory observations also reveal that the instability wave initiated has a wave number which corresponds to the maximum amplification rate according to stability theory. For the value of the Richardson number taken, we therefore take the initial disturbance with a wave number $\alpha_1 = 0.5$. We have also investigated the effect of (small) Ri by performing calculations for $\mathrm{Ri} = 0$. It was found that the estimate of billow lifetime, to be discussed subsequently, is not affected by variations in Ri provided that Ri is "small". The explicit effect of Ri on the final equilibrium amplitude can be qualitatively seen from the analysis given in the Appendix.

The question naturally arises as to the value of the initial disturbance level one should specify in starting the numerical calculations. However, it is not possible to obtain such initial disturbance values in any exact or unique sense. In a stratified fluid, in contrast to a homogeneous fluid, the region external to the strong velocity shear and potential temperature stability layer in question makes possible the radiation of initiating disturbance signals from other remote regions of the fluid—that is, the triggering disturbance need not be physically present within the shear layer in question. Thus, it is difficult to discuss any such remote triggering sources uniquely. These could include the collapse of well-mixed regions (Wu, 1969), the provocation of inversion layers by thermals (Townsend, 1964, 1965), as well as the development and collapse of other regions of active finite amplitude Kelvin-Helmholtz instability, to mention a few possibilities. In the tilting tube experiments of Thorpe (1971, 1973*a*, *b*), however, the ambient fluid was not stratified. Fortunately, the initial disturbance level in our formulation $|A|_0^2$ is an integral quantity and therefore not particularly sensitive to the detailed vertical distribution of the initial disturbance level. It essentially expresses the ratio of the initiating disturbance kinetic energy to the kinetic energy of the driving mean velocity difference across the shear layer ΔU. If the initial root-mean-square velocity fluctuation, made dimensionless by ΔU, is approximately 10^{-2}, then $|A|_0^2 \sim 10^{-5} - 10^{-4}$ and

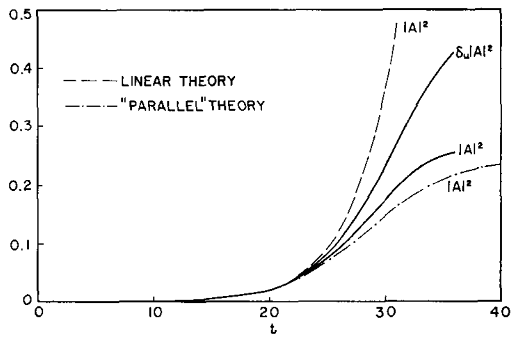

Fig. 2. Development of the dimensionless kinetic energy $\delta_u|A|^2$ and energy density $|A|^2$ of the Kelvin-Helmholtz wave. $\mathrm{Ri} = 0.08$, $\alpha_1 = 0.5$ and $|A|_0^2 = 10^{-4}$, $\delta_u(0) = \delta_\theta(0) = 1$.

this is of the same order as the initial noise levels in Thorpe's (1971) experiments which conceivably triggered the naturally-occurring Kelvin-Helmholtz instabilities. Of course, the amplifying system selects the wave number for which the growth rate is maximum. In the numerical application, $|A|_0^2$ is taken to be 10^{-4}. The initial δ_u and δ_θ are taken as equal in solving the nonlinear interaction problem (eqs. (19)–(21)) involving the development of the wave energy $\delta_u|A|^2$ and the growth of the velocity shear layer δ_u and potential temperature layer δ_θ. All the detailed considerations and comparison with observations, where possible, are made for this case. Subsequently, two special cases are considered in which (i) $\delta_u = \delta_\theta$ and eq. (21) is suppressed and (ii) $\delta_u = \delta_\theta = \text{constant}$, the parallel case. The conclusions regarding the mean flow modification and wave lifetime scale are not altered by these simplifying assumptions.

(*a*) *Development of instability wave energy, velocity shear and potential temperature layers*

The integrals I_{rs}, I_{hf}, I_{wt} defined in eqs. (22)–(24) are functions of the dependent variables δ_u and δ_θ through the dependence of the local eigenvalue problem (17) on the local parameters $\alpha = \alpha_1\delta_u$, $\mathrm{Ri}\,\delta_u r$. To simplify the numerical scheme for the integration of eqs. (19)–(21), the integrals are taken to be determined by their value at each preceding time step. Equations (19)–(21), subjected to the initial conditions already discussed, are then integrated numerically using a fourth-order Runge-Kutta method with step size $\Delta t = 0.5$.

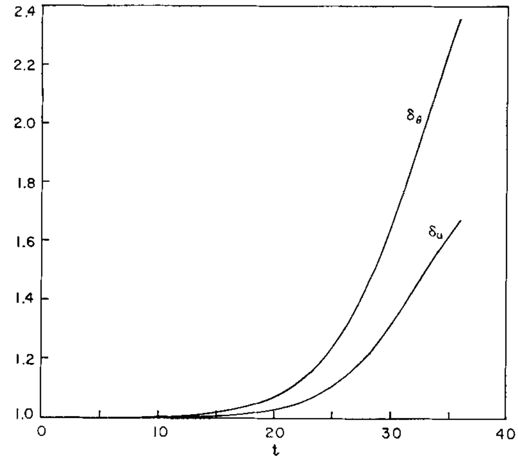

Fig. 3. Development of the mean velocity shear layer thickness δ_u and potential temperature layer thickness δ_θ. $\mathrm{Ri} = 0.08$, $\alpha_1 = 0.5$ and $|A|_0^2 = 10^{-4}$, $\delta_u(0) = \delta_\theta(0) = 1$.

The accuracy is checked by halving this step size. Recalling that the dimensionless time here is referred to δ_{u1}/U_1 or $(2\delta_{u1})/\Delta U$. Methods for solving the eigenvalue problem are described, for instance, by Maslowe & Kelly (1971) and by Hazel (1972).

The evolution of the dimensionless, averaged kinetic energy of the instability wave, $\delta_u |A|^2$, is shown in Fig. 2 by the solid line. Also shown by a solid line is $|A|^2$, the energy density. Initially, $|A|^2$ grows exponentially according to the linear theory, as indicated, but eventually becomes of sufficient finite amplitude that the growth is limited by the mechanisms already anticipated and discussed in connection with eq. (25). In the early stages, $\delta_u |A|^2$ follows $|A|^2$ when δ_u is still very near its initial value of unity. The time development of δ_u and δ_θ is shown in Fig. 3. Note that the temperature layer spreads faster than the shear layer. The reason for the limit in the growth of $|A|^2$ and the growth of δ_u and δ_θ can be more readily seen in the Fig. 4, in which the time development of the right-hand sides of eq. (19)–(21) is shown. The term $|A|^2 I_{rs}$ provides for the production of wave kinetic energy at the expense of the mean flow and is also responsible for the spread of the mean velocity shear layer according to eq. (20). The term $|A|^2 \mathrm{Ri}\, \delta_u I_{wt}$ provides the wave kinetic energy loss due to work against gravity, while $|A|^2 r I_{hf}$ is responsible for the spread of the mean potential temperature layer according to eq. (21). The development of $\delta_u |A|^2$ according to eq. (19) is determined by the net value of $|A|^2 (I_{rs} - \mathrm{Ri}\, \delta_u I_{wt})$. Now Fig. 4 indicates that all these source and sink terms grow exponentially during the early and intermediate stages of development, since $|A|^2$ itself grows exponentially, and the various integrals are nearly constant because there δ_u and δ_θ are very nearly constant. As δ_u, δ_θ grow to values significantly larger than the initial values of unity, the integrals I_{rs}, I_{wt} and I_{hf} decrease rapidly. This behavior is attributed to the dependence of the local eigenvalue problem on δ_u and δ_θ: as they increase, the local amplification rate decreases rapidly and the integrals also decrease rapidly. The physical reason is that as the local wave behavior evolves from one of large growth rates to one of small growth rates, the wave energy production mechanism, among other transfer mechanisms, significantly weakens. The evolution of the local eigenvalues is shown in Fig. 5, where $J_{\mathrm{MIN}} = \mathrm{Ri}\, \delta_u$,

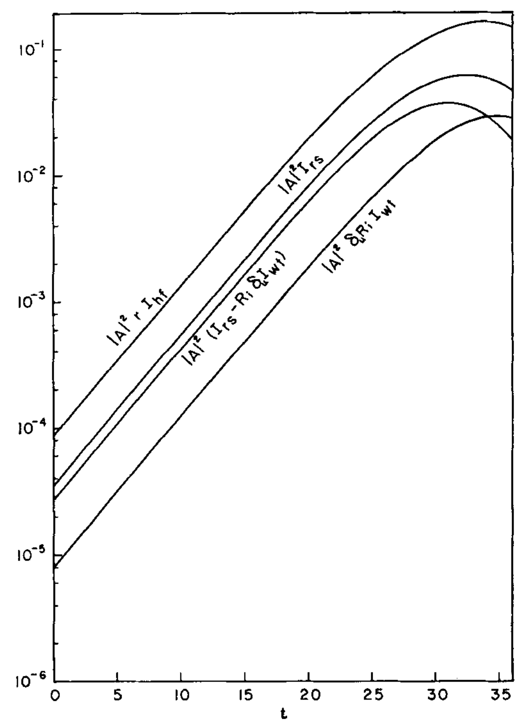

Fig. 4. Development of energy balancing mechanisms. $\mathrm{Ri} = 0.08$, $\alpha_1 = 0.5$ and $|A|_0^2 = 10^{-4}$, $\delta_u(0) = \delta_\theta(0) = 1$.

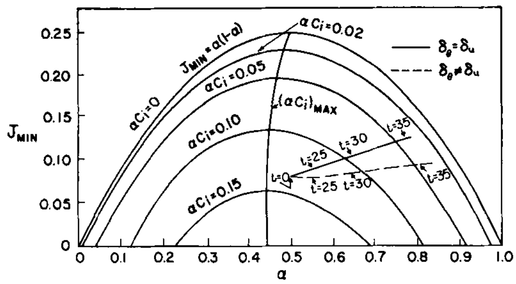

Fig. 5. The stability plane according to the linear theory for $\delta_\theta = \delta_u$. Superimposed are lines showing evolution of the local eigenvalue problems on this plane.

$\alpha = \alpha_1 \delta_u$, and αC_i is the amplification rate. The disturbance is initiated at $t = 0$ and the evolution in time is appropriately shown.

Thorpe (1971, 1973*a*, *b*) observed that billow breakdown takes place at about the time when the amplitude of the wave has reached a "saturated" value. The lifetime of the wave can be indicated by the saturation of the amplitude $|A|^2$ in the present calculations. This is physically reasonable because at this stage the energy supply from the mean motion is significantly weakened. Our result shows that this takes place at about 35 to 50 units of $2\delta_{u1}/\Delta U = \delta_{u1}/U_1$, where δ_{u1} and U_1 are the initial half width and half velocity difference. Estimating the development time between wave slopes of about 0.2 to about 1.25 when breaking occurs, Thorpe (1971, 1974) gives $21(2\delta_{u1})/\Delta U$, which would also be close to our estimation if Thorpe's growth time from smaller slopes (if known) were added. The observations of Browning & Watkins (1970) of the event over Pershore, 1243 GMT, 6 February 1970 show that the shear $\partial\bar{U}/\partial z$ was $4 \times 10^{-2}\,\mathrm{sec}^{-1}$ over a layer of 400 m and $3/8 \times 10^{-2}\,\mathrm{sec}^{-1}$ over a layer of 800 m, so that the "lifetime" of the wave development should be 35 to 40 times $10^2/4$ or about 15–17 minutes. Their observations indicate that the time scale is about 15 minutes. The instabilities observed by Woods (1968) and Woods & Wiley (1972) are attributed to the intensification of the local velocity shear by an internal wave superimposed on the geostrophic shear, as anticipated by Phillips (1966). For Woods & Wiley's (1972) observations in the Mediterranean thermocline, $\Delta U \simeq 2.2 \times 10^{-2}$ m/s and $2\delta_{u1} \simeq 10^{-1}$ m to 2×10^{-1} m so that our estimation gives about 3 to 6 minutes compared to their observed lifetime of 5 minutes for individual mixing events. At the end of this development time, our calculations indicate that both δ_u and δ_θ have doubled their initial values. Again, this is in accordance with observations (Browning & Watkins, 1970; Woods & Wiley, 1972).

(*b*) *Vertical momentum and heat fluxes*

The vertical flux of horizontal momentum and the vertical heat flux (averaged over one horizontal wave length) is obtained from eq. (16), where all quantities are now known:

$$-\overline{uw} = |A|^2 i\alpha(\phi\tilde{\phi}' - \tilde{\phi}\phi'),$$

$$-\overline{w\theta} = |A|^2 i\alpha(\phi\tilde{\tau} - \tilde{\phi}\tau)$$

Here $|A|^2$ is time-dependent only and the remaining factors, obtained from the *local* eigenvalue problem, depend on time and have a vertical distribution. It is the vertical distribution that is of particular interest. Thus, in Fig. 6 we show $-\overline{uw}/|A|^2$ and $-\overline{w\theta}/|A|^2$ for $\alpha = 0.5$ which corresponds to our $t = 0$ shape distribution. Subsequent distributions are qualitatively the same. Both of the functions are symmetric about $z = 0$ (because of the mean flow distribution). The heat flux function is considerably larger than the momentum flux function. This is primarily because, from the energy equation, the potential temperature shape function τ behaves as $\Theta_l'\phi/(U - c)$ according to the local linear theory. Near $z \approx 0$, the mean velocity and the complex phase

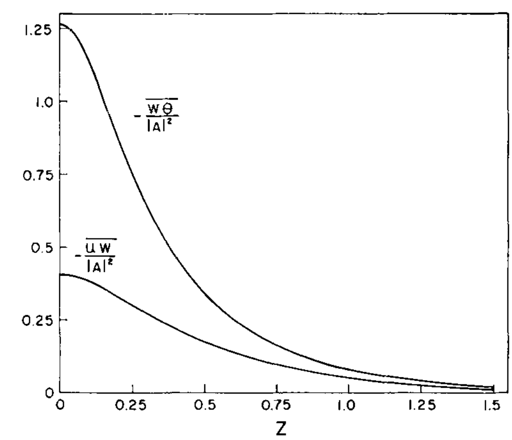

Fig. 6. Shape function distribution for the Reynolds stress $-\overline{uw}/|A|^2$ and vertical heat flux $-\overline{w\theta}/|A|^2$ for Ri $= 0.08$, $\alpha = 0.5$, $\delta_u = \delta_\theta$.

speed differs by a factor iC_i, where $C_i<1$ even for the most amplified initial disturbance (see Fig. 5). Since these vertical fluxes are responsible for redistributing the mean flow momentum and potential temperature (see eqs. (5) and (7), respectively), then according to these results it is not surprising that the mean potential temperature is more significantly affected by the passage of the wave than the mean velocity, as we shall see in the next section. Indeed, this was noted by Browning & Watkins (1970) in their Pershore observations. What is more interesting is that $\overline{w\theta}<0$, that is, the wave effects a downward heat flux, from regions of high to regions of low mean potential temperature. Such a downward heat transfer associated with a dominant wavelength of major and secondary billows was observed by Browning et al. (1973) shortly after 1900 GMT on 10 May 1972 above Defford in connection with a strongly sheared frontal region just below a jet axis.

(c) *Modifications of the mean velocity and potential temperature distributions by the wave*

Once the overall evolution problem is solved, it is then possible to "correct" the mean flow, as discussed earlier, by assessing the permanent "impressions" left upon it by the passage of the wave as it grows into finite amplitude. The correction to the mean velocity distribution has been taken to be U_m, where

$$\bar{U} = \tanh\frac{z}{\delta_u(t)} + U_m(z, t) \tag{27}$$

and it is U_m which we seek here. According to eq. (5), after the substitution of (27), we obtain

$$\frac{\partial U_m}{\partial t} = \frac{1}{\delta_u}\frac{\partial - \overline{uw}}{\partial \zeta} + \zeta \operatorname{sech}^2 \zeta \frac{d \ln \delta_u}{dt} \tag{28}$$

which gives, upon substituting the shape functions (16) into eq. (28),

$$U_m = \int_0^t |A|^2 \frac{i\alpha}{\delta_u}(\phi\tilde{\phi}' - \tilde{\phi}\phi')'\, d\bar{t} + \zeta \operatorname{sech}^2 \zeta \ln \delta_u \tag{29}$$

Similarly, the corrected mean potential temperature distribution has been taken to be

$$\bar{\Theta} = \tanh r\frac{z}{\delta_u(t)} + \Theta_m(z, t) \tag{30}$$

and accordingly, from eq. (7), (16) and (30),

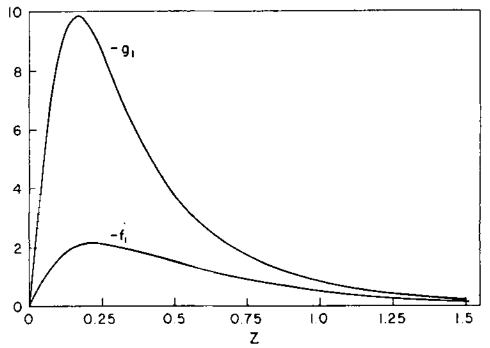

Fig. 7. Shape function distribution for the vertical gradient of the Reynolds stress $-f_1 = (\partial - \overline{uw}/\partial z)/|A|^2$ and of the vertical heat flux $-g_1 = (\partial - \overline{w\theta}/\partial z)/|A|^2$ for Ri = 0.08, $\alpha = 0.5$, $\delta_u = \delta_\theta$.

$$\Theta_m = \int_0^t |A|^2 \frac{i\alpha}{\delta_u}(\phi\tilde{\tau} - \tilde{\tau})'\, d\bar{t} + r\zeta \operatorname{sech}^2 r\zeta \ln \delta_\theta \tag{31}$$

recalling that $r(t) = \delta_u/\delta_\theta$.

The modification of the mean flow by the wave is achieved by the processes described in eqs. (29) and (31). The last terms in eqs.

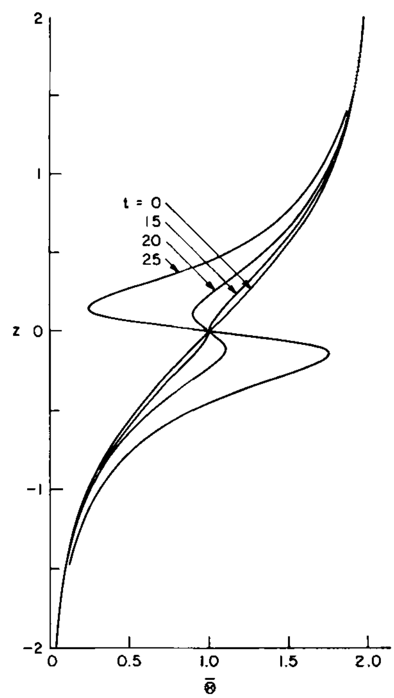

Fig. 8. Development of modified mean potential temperature distribution due to wave occurrence. Ri = 0.08, $\alpha_1 = 0.5$ and $|A|_0^2 = 10^{-4}$, $\delta_u(0) = \delta_\theta(0) = 1$.

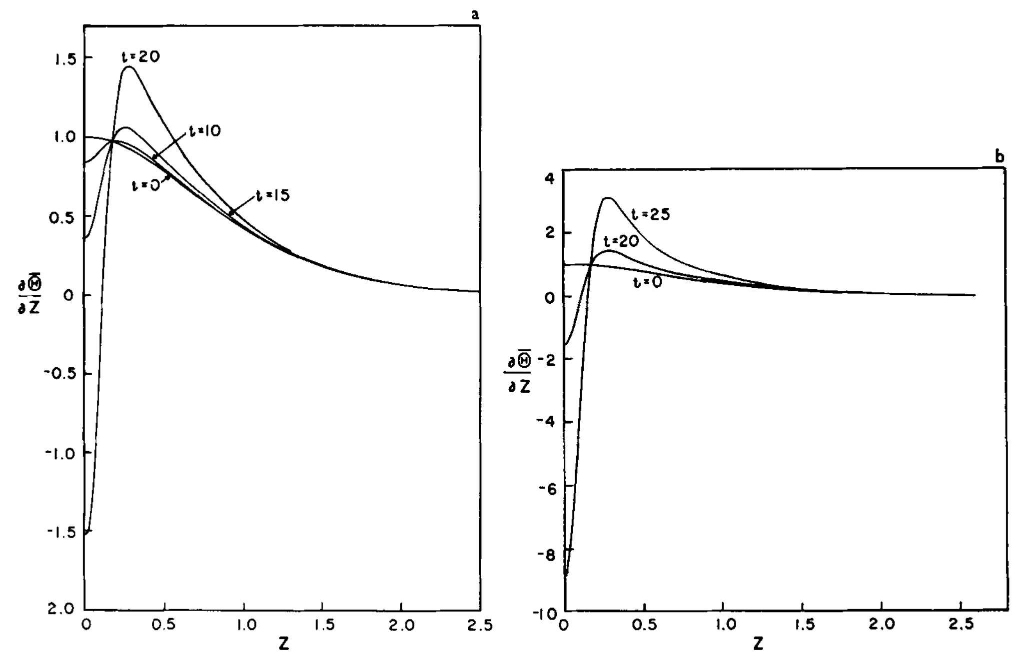

Fig. 9. Development of modified mean potential temperature gradient due to wave occurrence. Ri $= 0.08$, $\alpha_1 = 0.5$ and $|A|_0^2 = 10^{-4}$, $\delta_u(0) = \delta_\theta(0) = 1$. (*a*) Early stages. (*b*) Later stages.

(29) and (31), of the form $\zeta\,\mathrm{sech}^2\,\zeta \ln \delta_u$, are opposite in sign to the respective first terms which are the momentum and heat fluxes. However, the latter essentially provide the main character and dominate the correction. It is therefore of interest to look first at the vertical gradient of such fluxes. Fig. 7 shows the shape function distribution of $-f_1 = (\partial \overline{uw}/\partial z)/|A|^2$ and $-g_1 = (\partial \overline{w\theta}/\partial z)/|A|^2$ for the same conditions as the momentum and heat fluxes in Fig. 6. Both $-f_1$ and $-g_1$ are antisymmetric about $z = 0$. Again, Fig. 7 tells us that the modifications to the mean potential temperature are more noticeable than those to the mean velocity profile, in accordance with observations (Browning & Watkins, 1970). The mean potential temperature, modified by the wave induced heat flux according to eq. (31), is shown in Fig. 8. At dimensionless time $t = 20$ and 25, we see that $\bar{\Theta}$ has suffered major modifications (but only slightly for $\bar{U}$ as indicated by results not presented in this paper). Recently, laboratory measurements by Wang (1975) provide a velocity profile that is very similar to our modified mean velocity profile which is qualitalively the same as Θ in Fig. 8.

The early and later stages of the development of the modified mean potential temperature gradient profile $\partial\bar{\Theta}/\partial z$ are shown in Figs. 9*a* and *b*. At $t = 0$ we start with a profile that has a single maximum which eventually splits into two maxima while the central region was less stable, as Browning & Watkins (1970) observed. However, at later stages the central region develops into a gravitationally unstable one. In addition to the observation of multiple positive temperature gradient layers discussed by Woods & Wiley (1972), they also reported observations of regions of large ($\leqslant 250$ mK dm^{-1}) negative temperature gradients. At $t = 20$ from our Fig. 9*a*, for instance, the dimensionless negative gradient in the central region is approximately 2. If we take the original $2\delta_{u1}$ to be 1 dm and $\Delta\Theta$ to be 100 mK, then gradients of that same order of magnitude are obtained from our estimation. It is difficult to tell whether local regions of static instability existed or not in the absence of simultaneous salinity data. However, the present considerations indicate that such regions could exist, as a result of Kelvin-Helmholtz instability, but in the presence of a mean shear as well.

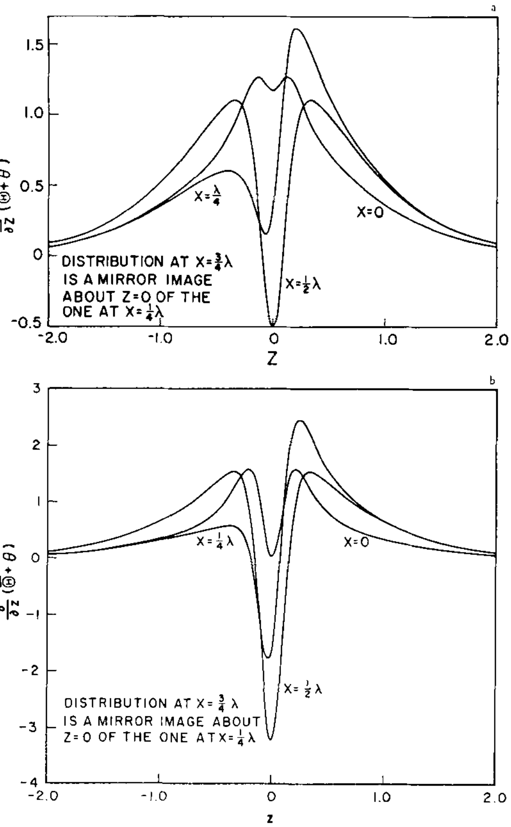

Fig. 10. Instantaneous vertical distributions of the total potential temperature gradient for various horizontal locations within the billow wavelength λ. $\mathrm{Ri} = 0.08$, $\alpha_1 = 0.5$ and $|A|_0^2 = 10^{-4}$, $\delta_u(0) = \delta_\theta(0) = 1$. (*a*) $t = 15$. (*b*) $t = 20$.

(d) The total potential temperature gradient distributions

So far we have discussed modified mean profiles. However, we shall see that the total instantaneous signal is also of interest. In field measurements the probe is sent to sample the vertical distribution as the wave is possibly advected by the meso-scale system. In this case, it is not possible to obtain a true vertical cross-section, in contrast with observations in which the probe is identically following the wave. Even if this difficulty is overcome, the averaging procedure in obtaining the mean flow is difficult because of the large number of data points needed. It would thus be helpful towards interpreting field and laboratory observations if we showed the total instantaneous profiles of, say, the potential temperature gradient. In Figs. 10*a* and *b* are shown the $t = 15$ and 20 instantaneous vertical distributions of the total potential temperature gradient profiles for various locations within the horizontal billow wavelength λ. This is obtained by summing vertical derivatives of the distribution $\bar{\Theta}$ (eq. (30)) and θ (eq. (16)). At $t = 15$, for the mean profile corresponding to the one in Fig. 9*a*, the total component at different horizontal locations together could be drastically different from the mean profile. While at this instant the mean profile is statically stable throughout, the total profile gives instantaneous gravitationally unstable regions, mainly in the central region about $z = 0$. Fig. 10*b* shows the total profiles at $t = 20$ corresponding to the mean profile given in Fig. 9*b*. Again, both the maxima and minima are accentuated. In both cases, the $x = 0$ location qualitatively resembles the original mean profile. We note that over the vertical scale relevant to our analysis θ_0, the hydrostatic component, can be taken as constant.

The potential temperature distribution in the formulation here is essentially similar to the density distribution in the laboratory observations of Thorpe (1973*a*, *b*) who used a conductivity probe to obtain the vertical density distributions. The mean (horizontally averaged) profile is not obtainable from such a single vertical traverse, however, the profile so obtained would be the total (mean plus wave) instantaneous density profile according to the present interpretations. Just prior to the breakdown of the ordered motions, a large scale zigzag occurred in the total density profile (Thorpe, 1973*a*, Fig. 8*a*) whose vertical gradient strikingly resembles the total potential temperature gradient shown in our Fig. 10 for advanced stages of billow development, with the central region being gravitationally unstable. The multiple sheets observed by Woods & Wiley (1972) could also correspond to the total instantaneous profiles, if the wave still exists. The tendency of multiple-sheet formation is amply suggested by our Fig. 10. However, sheet formation of a "permanent" form is reflected by the mean profiles, Fig. 9, which persist long after the collapse of the instantaneous wave profiles.

(e) The billow vertical velocity

The analysis is intended to provide simultaneous development of $|A|^2$, δ_u and δ_θ from the vertically integrated conservation equations.

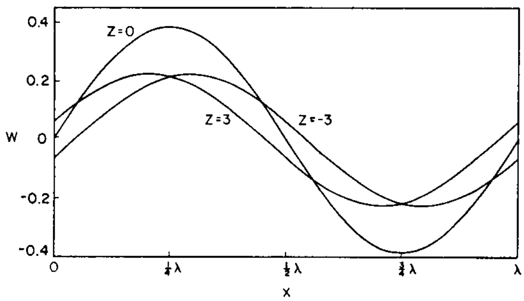

Fig. 11. Horizontal distribution of the billow vertical velocity at different vertical positions. Ri = 0.08, $\alpha_1 = 0.5$, $|A|_0^2 = 10^{-4}$, $\delta_u(0) = \delta_\theta(0) = 1$ at $t = 35$.

Such an approach is insensitive to the assumed shape functions which are here taken to be given by the local linear theory. However, just as in the modified mean flow development, some estimates of the vertical velocity can be obtained through the shape function, eq. (16). The integral theory gives only $|A|^2$, but the phase of A can be obtained through the recognition that following the billow, the billow wave speed is zero, and thus A would be real. We show in Fig. 11 the vertical billow velocity at a mature stage corresponding to $t = 35$. The vertical distribution is very nearly even—that is, w decays rather slowly away from the mean shear region. To obtain the dimensional vertical velocity, we recall that w is made dimensionless by $U_1 = \Delta U/2$. If we consider Browning & Watkins' (1970) observations as an example, Fig. 11 tells us that at the outer edges of the layer the vertical velocity is about 1/2 ms^{-1}, while at the center of the billow this velocity is about 1 ms^{-1} corresponding to a case of "moderate" clear-air turbulence based on a $\Delta U \sim 4$ m/s. In order to compare with the observations of Browning et al. (1973), an estimate of the initial data δ_{u1} and $\Delta U/2$ need to be made. The billows which they observed are in a mature stage and the wind shear is about 16 ms^{-1} over 400 m. It is not unreasonable to estimate that the initial echo layer from which the billows developed might be about 100 m and that $\Delta U \sim 4$ ms^{-1} (using Browning & Watkins (1970) as a guide). In this case, the vertical location of their aircraft observations of w from the center of the billow would be about $z \approx 1$ according to our Fig. 11 from which the dimensional $w_{\max} \approx 0.35(\Delta U/2) \approx 0.7$ ms^{-1}, which is consistant with the $w_{\max}$ associated with the observed *ordered* motions of Browning et al. (1973, Fig. 4). The main result of Fig. 11 is to show that the violent billow vertical velocity decays rather slowly in the vertical direction from its center.

4. Discussion

The total signals (shown in Fig. 10) are not as significant for future events as the mean distribution (Fig. 9) in that the wave component ultimately decays and its instantaneous influence ceases, whereas the modified mean flow remains. Thus, it is more significant to discuss a gradient Richardson number distribution $J(z, t)$ in terms of the *modified* mean profiles for the purpose of searching for new sites of dynamical instability resembling the original shear layer. The time development of J is shown in Fig. 12. The original gradient Richardson number is $J(z, t = 0)$ and the minimum is given by Ri = 0.08. The site of the original gravitationally-stable minimum is shifted away from the central region at $z = 0$, and at $t = 25$ the new location of this minimum is at a distance of about one half δ_{u1} where inflexional points in the mean velocity profile develop. The value of the stable minimum Richardson number is still considerably lower than the critical value of 1/4, so that it is reasonable to expect that these outer regions are new sites for dynamical instability similar to the original instability. Thus, such dynamical instabilities and

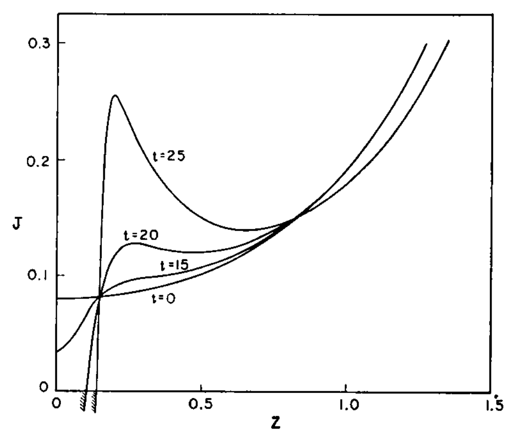

Fig. 12. Development of the wave-modified mean gradient Richardson number. Ri = 0.08, $\alpha_1 = 0.5$ and $|A|_0^2 = 10^{-4}$, $\delta_u(0) = \delta_\theta(0) = 1$.

splitting are self-generating in the sense that the instabilities "permanently" modify the original mean flow so that future instabilities and splitting may occur. This process is entirely different from and unrelated to harmonic generations from the original fundamental component. New, smaller-scale instabilities away from the central region of the original billows were observed by Gossard et al. (1970) in the 19 July 1969, 0100 PST event above the San Diego Bay and also by Browning & Watkins (1970). This self-generating mechanism has also been conjectured by Woods & Wiley (1972) and Woods (1972), and our analysis lends rational support to that conjecture.

In Fig. 12, the central region eventually develops into a gravitationally unstable one. One can conjecture that this may be the site from which turbulence originates which leads to the engulfing and breakdown of the billow. However, the problem of a simultaneously occurring strong shear and gravitationally unstable region remains to be studied. From our results, it appears that the large-scale splitting of the original statically stable layer is to be entirely attributed to the large-scale organized wave effects. This would be physically more appealing than to attribute splitting to the smaller-scale motions. The latter would be more likely to be responsible for smoothing the large-scale inhomogeneities, rather than their cause. It is conceivable that such gravitationally unstable regions could have existed in the Pershore observations of Browning & Watkins (1970). However, the gravitational instability could easily be missed between their successive hourly radio ascents because presumably it is of short duration. On the other hand, according to our results, a vertical resolution of about 50 m would be required for its detection.

Splitting might not occur if the instability wave cannot achieve sufficient amplitudes to effect the mean motion. This would be the case if the wave were initiated at significantly lower energies, if dissipative mechanisms were sufficiently strong so as to prevent its growth to large amplitudes, and if the time scale of the large scale mean motion were insufficient for the wave to develop.

If the initial mean velocity and potential temperature profiles were displaced relative to one another, one would expect an appropriate asymmetry in the eigenfunction profiles and a corresponding asymmetrical modification of the mean profiles. If the mean profiles were asymmetrical, then the major effect is a propagating phase speed (rather than zero in the coordinate system here) as found by Hazel's (1972) calculations using the linear theory, however, the growth rates remain the same. Hazel (1972) also found that when $\delta_{\theta 1} < \delta_{u1}$, the flow would be unstable for some α no matter how large Ri may be and these are propagating modes. However, their growth rates for large Ri are small, and for a fixed Ri $< 1/4$ are smaller than the "conventional" non-propagating modes. One thus expects that as far as observations of natural events are concerned, the overall behavior is still given by the non-propagating modes.

On the basis of such approximate considerations, we have attempted to explain certain features in the development of Kelvin-Helmholtz billows observed in the atmosphere, ocean and laboratory. These include the overall features: the billow "lifetime" and the doubling of the shear layer thickness, both of which are not sensitive to the details of the shape assumption. As far as the details are concerned, at least during the initial stages the linear shape functions of the wave made for the integral problem are not far removed from the actual situation and this shows that there certainly exists the tendency for the splitting of the temperature gradient layer attributed to the downward heat flux generated by the wave. At large amplitudes this direction of heat flux still persists according to observations (Browning et al., 1973). The estimate of the vertical billow velocity at maturity is more dependent on the "equilibrium" amplitude obtained from the integral problem rather than the details. Clearly, not all the observed features are explained (nor is their explanation intended within such a greatly simplified framework). The possible role of the small-scale oscillations in arresting the development of the large-scale wave is yet to be understood. Certain observed detailed features of such small-scale motions appear to be mini-Kelvin-Helmholtz instabilities, while others seem to be random motions. The study of the interactions of the disparate large- and small-scale motions is certainly of great interest to the understanding of this problem. Such studies will be reported elsewhere (Liu & Merkine, 1976).

Acknowledgments

We should like to acknowledge various helpful discussions or communications that one of us (J. T. C. L.) has had with D. N. Axford, K. A. Browning, J. S. A. Green, R. F. Probstein, J. H. Richter, J. T. Stuart, S. A. Thorpe and J. D. Woods; and to acknowledge the hospitality of the Department of Mathematics, Imperial College, London enjoyed by J. T. C. L. during the early stages of this work. Some aspects of this work were first presented at the American Physical Society 26th Annual Division of Fluid Dynamics Meeting, 19–21 November 1973 at Yale University (Liu & Merkine, 1973) and at the I.A.P.S.O. Symposium on Ocean Microstructure, XVI I.U.G.G. General Assembly, 25 August–6 September 1975 in Grenoble, France (Liu, 1975). The research reported in this paper is supported by the Fluid Dynamics Program, Office of Naval Research, United States Navy through Contracts No. N00014-67-A-0191-0022, Identifying No. NR 061-204, and No. N00014-76-C-0363, Identifying No. NR 062-530.

Appendix

The results discussed in the main text of the paper are obtained from the simultaneous solution of eqs. (19)–(21) for $|A|^2$, δ_u and δ_θ. Here we consider some special cases by suppressing one and then two of the three dependent variables and their respective equations.

(i) *The $\delta_u = \delta_\theta$ case ($r = 1$)*

In this special case, eq. (21) is suppressed and replaced by forcing $\delta_\theta = \delta_u$. Only eqs. (19) and (20) are jointly solved. In this case, the linear stability characteristics are well known (see for instance, Maslowe & Kelly, 1971). The evolution of the problem in the J_{MIN} vs. α plane for this case is shown as a solid line in Fig. 5. The "final" thickness of the layer can be obtained without carrying the integrations through. Since $J_{\mathrm{MIN}} = \mathrm{Ri}\,\delta_u$ and $\alpha = \alpha_1\delta_u$ at each instant, at equilibrium on the neutral curve $\mathrm{Ri}\,\delta_{ue} = \alpha_1\delta_{ue}(1-\alpha_1\delta_{ue})$ from the known stability boundary. Thus, $\delta_{ue} = (1-\mathrm{Ri}/\alpha_1)/\alpha_1$. For $\alpha_1 = 0.5$ and $\mathrm{Ri} = 0.08$, $\delta_{ue} = 1.68$. The results at $t = 35$ indicate that already $\delta \simeq 1.55$. Except for minor details the mean profile modifications resemble those of the $\delta_u \neq \delta_\theta$ case.

(ii) *The parallel shear layer*

Here both eqs. (20) and (21) are suppressed and $\delta_u = \delta_\theta = 1$; only eq. (19) is solved for $|A|^2$. For a homogeneous shear flow, the idea dates back to Stuart (1958). In this case, the shape functions remain frozen at their initial values. Because of their simplicity, the modifications of the mean flow through the production term can be easily accounted for in the vertically integrated equation, eq. (19).

Keeping in mind that $\delta_u = \delta_\theta = 1$, upon substitution of the corrected mean velocity, eq. (27), into the production term in eq. (19), we obtain

$$\frac{d|A|^2}{dt} = (I_{rs} - \mathrm{Ri}\, I_{wt})\,|A|^2 - 2\alpha c_i I_{\mathrm{mod}}|A|^2 \int_0^t |A|^2 d\bar{t} \tag{32}$$

where $I_{\mathrm{mod}} = 2\alpha c_i \int_{-\infty}^{\infty} f_1^2 dz$, and I_{rs}, I_{wt} and f_1 take the forms described previously. All the coefficients of eq. (32) are now time-independent. If we set $a = I_{rs} - \mathrm{Ri}\, I_{wt}$ and $b = 2\alpha C_i I_{\mathrm{mod}}$, eq. (32) can be written as

$$\frac{d|A|^2}{dt} = a|A|^2 - b|A|^2 \int_0^t |A|^2 d\bar{t} \tag{33}$$

which should be supplemented by the initial condition that

$$\text{at } t = 0,\ |A|^2 = |A|_0^2 \tag{34}$$

Eq. (33) can be converted to the second-order differential equation

$$|A|^2 \frac{d^2|A|^2}{dt^2} - \left(\frac{d|A|^2}{dt}\right)^2 + b|A|^6 = 0 \tag{35}$$

with the additional initial condition that

$$\text{at } t = 0,\quad \frac{d|A|^2}{dt} = a|A|_0^2 \tag{36}$$

Eq. (35) can again be converted with the aid of eqs. (36) and (34) into the following first-order equation;

$$\frac{d|A|^2}{dt} = |A|^2[a^2 - 2b(|A|^2 - |A|_0^2)]^{1/2} \tag{37}$$

Eq. (37) shows that there exists a maximum amplitude given by

$$|A|^2_{\max} = \frac{a^2}{2b} + |A|_0^2$$

The maximum amplitude depends on the initial amplitude except when $|A|_0^2 \to 0$. Eq. (37) also indicates that when $|A|^2 \to |A|_0^2$, the amplitude grows exponentially according to the linear theory, but independently of the value of $|A|_0^2$. Eq. (37) has the property that it follows a closed loop in the $(d|A|^2/dt,\ |A|^2)$ phase plane. This fact is physically unrealistic. Our previous discussion predicts a wave which develops into a neutral finite-amplitude stage. In this neutral stage there is no energy exchange between the wave and the mean flow, and in an inviscid flow the amplitude of the wave remains fixed. Eq. (37) has some resemblance to an equation derived by Drazin (1970) which also predicts that the wave traverses a closed path in the phase plane. On the other hand, the weakly nonlinear theory according to Stuart (1960) when applied to our case (given in detail in Appendix to Part II of Merkine, 1974) predicts an approach to equilibrium given by a first order differential equation for $|A|^2$, as does the energy integral consideration of the previous sections. In view of this discussion we shall attempt to simplify eq. (33). From Sec. 2 we know that

$$\frac{d|A|^2}{dt} = a|A|^2 + O(|A|^4)$$

Then, if we replace $|A|^2$ under the integral sign in eq. (33) by $|A|^2$ from above, keep terms up to order $|A|^4$ and assume that $|A|_0^2 \to 0$, the following equation is obtained:

$$\frac{d|A|^2}{dt} = I_{rs}|A|^2 - I_{\text{mod}}|A|^4 - \text{Ri}\, I_{wt}|A|^2 \tag{38}$$

The first two terms on the right-hand side of eq. (38) state that as the amplitude of the wave increases and the mean flow becomes more and more distorted, less energy via shear becomes available to the wave. The last term indicates the work done against gravity.

The *form* of the Landau equation, (38), first derived by Stuart (1958, 1960) under different circumstances, admits the closed-form solution

$$\frac{|A|^2}{|A|_0^2} = \frac{\exp\,(I_{rs} - \text{Ri}\, I_{wt})\,t}{1 + |A|_0^2 \dfrac{I_{\text{mod}}}{(I_{rs} - \text{Ri}\, I_{wt})}\,[\exp\,((I_{rs} - \text{Ri}\, I_{wt})\,t) - 1]} \tag{39}$$

which has the following properties:

(*a*) at $t = 0$, $|A|^2 = |A|_0^2$,

(*b*) as $t \to 0$, $\dfrac{|A|^2}{|A|_0^2} \sim \dfrac{\exp\,(I_{rs} - \text{Ri}\, I_{wt})\,t}{1 - |A|_0^2 \dfrac{I_{\text{mod}}}{I_{rs} - \text{Ri}\, I_{w'}}}$

indicating the exponential behavior required by the linear theory;

(*c*) as $t \to \infty$, $|A|^2 \to |A|_{eq}^2 = \dfrac{I_{rs} - \text{Ri}\, I_{wt}}{I_{\text{mod}}}$

In other words, an asymptotic equilibrium amplitude is obtained, and this amplitude is independent of the initial value of $|A|_0^2$.

Under the same approximation, the modifications of the mean flow are

$$\bar{U} = U_l + 2\alpha C_i f_1 |A|^2,$$

$$\bar{\Theta} = \Theta_l + 2\alpha C_i g_1 |A|^2$$

where g_1 has the form described previously.

In order to obtain numerical results, we use the same initial data as in Sec. 2: $\alpha_1 = 0.5$, $\text{Ri} = 0.08$, $I_{rs} - \text{Ri}\, I_{wt} = 2\alpha C_i = 0.2744$, $|A|_0^2 = 10^{-4}$ and $I_{\text{mod}} = 1.120$. Fig. 2 compares the development of the amplitude given by eq. (39) (called "parallel") to that given by the non-parallel case of Sec. 2. The approach to equilibrium of the "parallel" model is less rapid than that obtained from the previous cases of the growing shear layers. Nevertheless, the time scale and the final value of $|A|^2$ are both quite close. The development of the mean potential temperature stability profile again greatly resembles those for the $\delta_u \neq \delta_\theta$ and the $\delta_u = \delta_\theta$ cases.

REFERENCES

Atlas, D., Metcalf, J. I., Richter, J. H. & Gossard, E. E. 1970. The birth of "CAT" and microscale turbulence. *J. Atmos. Sci. 27*, 903–913.

Axford, D. N. 1970. An observation of gravity waves in shear flow in the lower stratosphere. *Quart. J. R. Met. Soc. 96*, 273–286.

Axford, D. N. 1973. On an observation of turbulent waves on the tropopause surface. *Quart. J. R. Met. Soc. 99*, 438–449.

Browning, K. A. 1971. Structure of the atmosphere in the vicinity of large amplitude Kelvin-Helmholtz billows. *Quart. J. R. Met. Soc. 97*, 283–299.

Browning, K. A. & Watkins, C. D. 1970. Observations of clear air turbulence by high power radar. *Nature 227*, 260–263.

Browning, K. A., Bryant, G. W., Starr, J. R. & Axford, D. N. 1973. Air motion within Kelvin-Helmholtz billows determined from simultaneous Doppler radar and aircraft measurements. *Quart. J. R. Met. Soc. 99*, 608–618.

Cox, C., Nagata, Y. & Osborn, T. 1969. Ocean fine structure and internal waves. *Bull. Japanese Soc. Fish. Oceanogr.* (Special Number, Prof. Uda's Commemorative Papers), pp. 67–71.

Drazin, P. G. 1970. Kelvin-Helmholtz instability of finite amplitude. *J. Fluid Mech. 42*, 321–335.

Dutton, J. A. 1971. Clear-air turbulence, aviation, and atmospheric science. *Revs. Geophys. and Space Phys. 9*, 613–657.

Gossard, E. E., Richter, J. H. & Atlas, D. 1970. Internal waves in the atmosphere from high resolution radar measurements. *J. Geophys. Res. 75*, 3523–3536.

Hardy, K. R., Atlas, D. & Glover, K. M. 1966. Multiwavelength backscatter from the clear atmosphere. *J. Geophys. Res. 71*, 1537–1552.

Hardy, K. R., Glover, K. M. & Ottersten, H. 1969. Radar investigations of atmospheric structure and CAT in the 3 to 20 km region. In *Clear air turbulence and its detection* (ed. Y. H. Pao and A. Goldburg), pp. 402–416. Plenum Press, New York.

Hardy, K. R., Reed, R. J. & Mather, G. K. 1973. Observation of Kelvin-Helmholtz billows and their mesoscale environment by radar, instrumented aircraft, and a dense radiosonde network. *Quart. J. R. Met. Soc. 99*, 438–449.

Hazel, P. 1972. Numerical studies of the stability of inviscid stratified shear flows. *J. Fluid Mech. 51*, 39.

Hicks, J. J. & Angell, J. K. 1968. Radar observations of breaking gravitational waves in the visually clear atmosphere. *J. Appl. Met. 7*, 114–121.

Kármán, Th. von 1921. Über laminare und turbulente Reibung. *Z. angew. Math. Mech. 1*, 233–252.

Ko, D. R. S., Kubota, T. & Lees, L. 1970. Finite disturbance effect in the stability of a laminar incompressible wake behind a flat plate. *J. Fluid Mech. 40*, 315.

Lilly, D. K. 1971. Progress in research on atmospheric turbulence. *EOS, Trans. Am. Geophy. U. 52*, IUGG 332–341.

Liu, J. T. C. 1975. Some aspects of microstructure formation by shear-induced instabilities and the propagation of internal waves in a microstructure. Abstract in *I.A.P.S.O. Scientific Program*, p. 87. XVI General Assembly, I.U.G.G. Grenoble, France.

Liu, J. T. C. & Lees, L. 1970. Finite amplitude instability of the compressible laminar wake. Strongly amplified disturbances. *Phys. Fluids 13*, 2932–2938.

Liu, J. T. C. & Merkine, L. 1973. On statically stable layer splitting in a stratified shear flow. Abstract in *Bull. Am. Phys. Soc. 18*, 1467.

Liu, J. T. C. & Merkine, L. 1976. On the interaction between large-scale coherent eddies and fine-grained turbulence in a free shear flow. Part I. *Proc. Roy. Soc.* (in press).

Liu, J. T. C. & Gururaj, P. M. 1974. Finite amplitude instability of the compressible laminar wake. Comparison with experiments. *Phys. Fluids 17*, 532–543.

Ludlam, F. H. 1967. Characteristics of billow clouds and their relation to clear air turbulence. *Quart. J. R. Met. Soc. 93*, 419–435.

Lumley, J. L. & Panofsky, H. A. 1974. *The structure of atmospheric turbulence.* Interscience Publ., New York.

Maslowe, S. A. & Kelly, R. E. 1971. Inviscid stability of an unbounded heterogeneous shear layer. *J. Fluid Mech. 48*, 405–415.

Mather, G. K. 1971. Flight studies of clear air turbulence—the current position and further research needs. In *International Conference on Atmospheric Turbulence*, Royal Aeronautical Society, London.

Merkine, L. 1974. *Problems in nonlinear mechanics of unstable waves in turbulent and in stratified shear flows.* Brown University, Division of Engineering, Ph.D. Thesis.

Metcalf, J. I. & Atlas, D. 1973. Microscale ordered motions and atmospheric structure associated with thin echo layers in stably stratified zones. *Boundary Layer Met. 4*, 7–35.

Munk, W. H. & Garret, C. J. R. 1973. Breaking and microstructure (the chicken and the egg). *Boundary Layer Met. 4*, 37–45.

Phillips, O. M. 1966. *Dynamics of the Upper Ocean*, p. 166. Cambridge University Press.

Scorer, R. S. 1972. *Clouds of the world.* David and Charles.

Stuart, J. T. 1958. On the nonlinear mechanics of hydrodynamic stability. *J. Fluid Mech. 4*, 1–21.

Stuart, J. T., 1960. On the nonlinear mechanics of wave disturbances in stable and unstable parallel flows. *J. Fluid Mech. 9*, 353–370.

Thorpe, S. A. 1971. Experiments on the instability of stratified shear flows-miscible fluids. *J. Fluid Mech. 46*, 299–319.

Thorpe, S. A. 1973*a*. Turbulence in stably stratified fluids: a review of laboratory experiments. *Boundary Layer Met. 5*, 95–119.

Thorpe, S. A. 1973*b*. Experiments on instability and turbulence in a stratified shear flow. *J. Fluid Mech. 61*, 731–751.

Thorpe, S. A. 1974. Private communication.

Townsend, A. A. 1964. Natural convection in water over an ice surface. *Quart. J. R. Met. Soc. 90*, 248–259.

Townsend, A. A. 1965. Excitation of internal waves by a turbulent boundary layer. *J. Fluid Mech. 22*, 241–252.

Wang, Y. H. 1975. An experimental study of the instability of a stably stratified free shear layer. *J. Fluid Mech. 71*, 563–575.

Woods, J. D. 1968. Wave-induced shear instability in the summer thermocline. *J. Fluid. Mech. 32*, 791–800.

Woods, J. D. 1972. Vertical mixing processes in the ocean. Conseil International pour l'Exploration de la Mer, *Extrait des Rapports et Procès-Verbaux 162*, 25–28.

Woods, J. D. & Wiley, R. L. 1972. Billow turbulence and ocean microstructure. *Deep-Sea Res. 19*, 87–121.

Wu, J. 1969. Mixed region collapse with internal wave generation in a density stratified medium. *J. Fluid Mech. 35*, 531–544.

ОПИСАНИЕ РАЗВИТИЯ ГРЯД КЕЛЬВИНА-ГЕЛЬМГОЛЬЦА С ПОМОЩЬЮ ИНТЕГРАЛА ЭНЕРГИИ

В этой статье мы изучаем развитие неустойчивых волн в стратифицированном потоке с поперечным сдвигом скорости, которые наблюдаются, например, во фронтальных зонах и на крупномасштабных волнах там, где число Ричардсона достаточно мало. Модель основывается на разбиении потока на среднее течение и неустойчивые волновые компоненты. Основой для взаимодействия между средним течением и волной являются соответствующие уравнения для потока энергии, проинтегрированные по вертикали. Описание волн получается путем предположения об их форме: зависящая от времени амплитуда волны определяется ее уравнением энергии, решаемым с привлечением среднего течения, а функция, описывающая форму волны по вертикали дается локальной линейной теорией. Кинетическая энергия неустойчивой волны определяется балансом между продукцией энергии из среднего потока и превращением флуктуационной кинетической энергии в потенциальную энергию. С точки зрения интеграла энергии численные результаты показывают сравнительно хорошее согласие с наблюдениями в нашей оценке времени жизни волны и в удвоении толщины слоя среднего сдвига в течение этого времени. Модификация профилей скорости и температуры среднего течения объясняется, соответственно, через эффекты генерации волной вертикальных потоков количества движения и тепла (или плавучести).